Department of Computer Science Technical Reports   Department of Computer Science

2001

Morphological and Physiological Effects of Mechanical Trauma to the Spinal Cord

Steven Teoh

Yinlong Sun

Report Number:
01-011

MORPHOLOGICAL AND PHYSIOLOGICAL EFFECTS OF MECHANICAL TRAUMA TO THE SPINAL CORD

Steven Teoh
Yinlong Sun

Department of Computer Sciences
Purdue University
West Lafayette, IN 47907

MORPHOLOGICAL AND PHYSIOLOGICAL EFFECTS OF MECHANICAL TRAUMA TO THE SPINAL CORD

Steven Teoh, Yinlong Sun
Department of Computer Science, Purdue University

Abstract

Spinal cord injury carries a high risk of mortality and morbidity. This report provides a summary of fundamental physiological aspects of the neuronal plasma membrane that are relevant to the study of spinal cord injury and a review of experimental animal models analyzing the morphological and physiological consequences of mechanical trauma to the spinal cord. There is currently no standardized method of inducing experimental spinal cord injury and quantifying the extent of injury. In general, the acutely damaged cord showed axonal compaction, periaxonal swelling and disruption of myelin sheaths. Weeks later, injured cords revealed a reduction in gray and white matter with progressively increasing axonal preservation toward the perimeter of the cords, a pattern attributable to the response of viscoelastic cord materials to mechanical impact. Degeneration of axonal function in both acute and chronic injury may be explained by damage to myelin sheaths and elemental derangement. Acute biochemical changes include an efflux of K^+ into the extracellular space and an intraaxonal influx of Na^+ and Ca^{2+}. Chronically elevated intraaxonal Ca^{2+} concentration appear to play an important role in cellular and myelin damage. The studies indicate that the ionic deregulation is mediated by a number of membrane channels as well as ionotropic glutamate receptors.

Keywords: Spinal cord injury, trauma, microscopy, histology, biochemistry, electrical conduction

Contents

1.   Introduction

Spinal cord injury (SCI) results in significant long-term individual and societal consequences. In the United States, figures provided by the National Spinal Cord Injury Statistical Center reveal a estimated of prevalence of 183,000 to 230,000 individuals living with trauma-related SCI and a incidence of about 10,000 new cases per year [McDonald99]. The injury is invariable debilitating; about 46% of the cases are either incomplete or complete paraplegic and about 53% are incomplete or complete tetraplegic [Nobunaga99]. Long-term secondary medical complications, such as pressure ulcers, pneumonia, deep vein thrombosis and renal calculi, contribute to the high healthcare expenses for individuals with SCI. The estimated costs of lifetime care for such an individual often exceed $1,000,000 and annual healthcare expenses average more than $5000 [McKinley99]. Significant impact of SCI, in terms of prolonged lengths of stay at rehabilitation centers, has also been reported in countries such as, Italy (130 days), Spain (140 days), Portugal (140 days) and Brazil (126 days) [Celani01]. In Australia, the high mortality and morbidity of SCI is revealed in a 1997 study of 132 SCI cases, among which 34% died in hospital and only 11% returned to work [Atkinson01]. The evidence from these studies undergird the importance of research to advance the understanding and management of SCI. The next two sections provide an overview of basic cell structure and physiology in the central nervous system relevant to the understanding of spinal cord injury at the cellular level. This is followed by a review of publications on experimental models used to study the morphological, physiological and functional effects of spinal cord injured induced in animals.

2.   Cells of the Central Nervous System

Cells of the central nervous system can be classified into two broad categories, namely, neurons and glial cells. Neurons are cellular units of the nervous system. They are specialized cells that receive and transmit electrical signals. Although neurons differ in morphology, they share the following basic features as shown in Figure 1:

- A cell body or soma, which synthesizes the components required for normal functioning of the neuron.
- Dendrites, cytoplasmic processes that transmit electrical signals to the soma
- An axon, a single cytoplasmic process that transmits electrical signals away from the soma. It may be encircled by concentric layers of myelin, collectively known as a myelin sheath. The latter is interrupted at intervals along its length by gaps known as nodes of Ranvier.

Unlike neurons, glial cells do not conduct electrical impulses. In general, they provide structural and functional support the neurons. Glial cells outnumber neurons by an approximate ratio of two to one. They occupy the space between neurons, reducing the extracellular space between cells to a width about 15 to 20 nm [Hammond01]. Different categories of glial cells are distinguished by their structure and function. Oligodendrocytes, for instance, form the myelin sheath surrounding axons as described above.

Cross-sections of the brain and spinal cord reveal that they both consist of regions with a darker color, known collectively as the gray matter, and regions of a lighter color, known as the white matter. The former is largely composed of neuronal cell bodies, while the latter contains neuronal cytoplasmic processes that conduct electrical signals.

3. The Neuronal Plasma Membrane

The neuronal plasma membrane is the outer covering of the neuron and serves as a boundary between the intracellular and extracellular fluid compartments. It is structurally similar to the plasma membrane of other cell types, that is, a bilayer of phospholipids with associated proteins (Figure 2). The phospholipid molecules form the backbone of the plasma membrane, each comprising a hydrophilic polar region and a hydrophobic nonpolar region. The hydrophilic regions of the phospholipids in each half of the bilayer are oriented away from the center of the bilayer while the hydrophobic regions are oriented toward the center. Protein molecules are attached to the inner or outer surfaces of the plasma membrane. Others, known as transmembrane proteins, extend through the width of the membrane.

3.1   Ionic Movement Across the Neuronal Plasma Membrane

The plasma membrane allows the passage of ions and molecules through various means as listed below [Cooper00]:

- Simple diffusion
- Facilitated diffusion
- Active transport

3.1.1   *Simple Diffusion*

Simple diffusion refers to the movement of ions or molecules down an electrochemical gradient directly through the lipid bilayer of the plasma membrane. No external source of energy is required. Nonpolar substances, such as oxygen and carbon dioxide, which are soluble in lipids, diffuse relatively fast. Small polar substances, such as water, may also diffuse through the lipid bilayer, but at a slower rate.

3.1.2   *Facilitated Diffusion*

Like simple diffusion, facilitated diffusion involves the movement of a substance down an electrochemical gradient without the need for an external source of energy. The difference is that facilitated diffusion is mediated by membrane proteins of which there are generally two categories: carrier proteins and channel proteins. *Carrier proteins* bind specific substances such as sugars, amino acids and nucleosides, located on one side of the plasma membrane. They then undergo conformational change, allowing the passage and release of these substances on the

other side of the membrane. In contrast, *channel proteins* form through which substances diffuse. Of importance to the neuronal plasma membrane are channel proteins known as ion channels, which mediate the diffusion of ions.

Among the ions present in the nervous system, sodium (Na^+), potassium (K^+), chloride (Cl^-) and calcium (Ca^{2+}) ions seem to account for almost all the ionic movements across the neuronal plasma membrane [Hammond01]. The ion channels play a crucial role in the transmission of electrical impulses through the neuron. Each ion channel has a central aqueous pore that exists in an opened or closed state. In the opened state, a channel allows the passage of ions across the plasma membrane while the closed state halts passage of ions. The process of opening or closing an aqueous pore is called *gating*. The latter results from changes to the channel's molecular conformation [Aidley96] as determined by specific stimuli. Ion channels may be classified according to their gating properties as shown in Table 1 [Hammond01]:

3.1.3 *Active Transport*

Unlike simple and facilitated diffusion, active transport involves the movement of molecules or ions against an electrochemical gradient and thus, requires the expenditure of energy, commonly provided by on the hydrolysis of adenosine triphosphate (ATP) by the enzyme ATPase. Ion pumps that maintain the electrochemical gradients across the plasma membrane are examples of active transport. For instance, the Na^+-K^+ ATPase pump transports Na^+ and K^+ ions across the membrane against their electrochemical gradients.

The transport of substances by membrane protein carriers, whether passive (facilitated diffusion) or active, may also be classified according to the number and direction in which substances are transported [Cooper00]:

- *Uniport*. The transport of a single type of substance across the membrane. An example of which is the facilitated diffusion of glucose.

- *Symport*. Also known as cotransport, it is the transport of two substances in the same direction. For example, the Na^+-glucose symport, which actively transports two Na^+ ions and one glucose molecule into the cell.

- *Antiport*. Also known as countertransport, it is the transport of two substances in opposite directions. For example, the Na^+-Ca^{2+} antiport, which actively moves Ca^{2+} and Na^+ ions in opposite directions. This antiport transports Ca^{2+} and Na^+ ions in either directions depending on the prevailing ion gradients and membrane potential [Li00].

3.2 The Membrane Potential

Passive movement of ions, namely, diffusion and electrophoresis, does not require the expenditure of energy. Electrophoresis refers to the movement of ions as a result of an electrical potential gradient across the plasma membrane, known as the *membrane potential*. The latter,

denoted by V_m, is the difference between the electrical potential of the intracellular compartment, V_i, and that of the extracellular compartment, V_e, (that is, $V_i - V_e$). The combination of diffusion and electrophoresis tends toward a state of equilibrium in ionic distribution across the plasma membrane as illustrated by the following example.

Compartments 1 and 2 in Figure 3 contain potassium ions, K^+ and anions, A^-. The membrane separating the compartments has an ion channel that allows only the passage of potassium ions and not the anions. The concentration of K^+ in compartment 1 is initially higher than that in compartment 2, causing the diffusion of K^+ from compartment 1 to 2. As the anions cannot cross the membrane, the excess positive charges in compartment 2 results in a electrical potential difference across the membrane which counteracts the diffusion of K^+ into compartment 2. A state of equilibrium is eventually reached in which the concentration gradient that tends to move the K^+ from compartment 1 to 2 is balanced by the electrical potential difference that tends to move the K^+ in the opposite direction. In this state, there is no further movement of K^+ across the ion channel and the membrane potential at this point is called the *equilibrium potential* or *Nernst potential* for potassium ions [Hammond01].

In general, when the membrane potential, V_m, equals the equilibrium potential of a particular ion, E_{ion} (that is, $V_m = E_{ion}$), there is no diffusion of the ion across the membrane. In contrast, when $V_m \neq E_{ion}$, diffusion of the ion occurs. The difference between V_m and E_{ion} (that is, $V_m - E_{ion}$) is called the *electrochemical gradient*. The value of the equilibrium potential for a particular ion, X, is given by the *Nernst equation* as shown:

$$E_X = \frac{RT}{zF} \ln \frac{[X]_1}{[X]_2}$$

E_X is the equilibrium potential in volts, R is the constant of an ideal gas (8.314 JK^{-1}mol^{-1}), T is the absolute temperature in kelvins, z is the valence of the ion, F is the Faraday constant (96500 C^{1}mol^{-1}) and $[X]_1$ and $[X]_2$ are the concentrations of ion X in the two compartments separated by the membrane.

The membrane potential of a neuron results from the composite distribution of multiple ionic species, namely, sodium, potassium and chloride ions, in the intrcellular and extracellular compartments. In the absence of electrical transmission, the neuronal membrane potential is at equilibrium and is called the *resting membrane potential*. A neuron typically has a resting membrane potential of between -60 mV and -80 mV. That is, the intracellular compartment has a negative potential with respect to the extracellular compartment. At this point, individual ionic species are not at equilibrium, that is, they continue to move across the plasma membrane. However, there is no net movement of electrical charge across the membrane. The resting membrane potential is derived from the Goldman-Hodgkin-Katz equation, which is similar to Nernst equation except that it simultaneously accounts for the contribution of various ionic species as shown:

$$E_m = \frac{RT}{F} \ln \left(\frac{p_K [K^+]_e + p_{Na} [Na^+]_e + p_{Cl} [Cl^-]_i}{p_K [K^+]_i + p_{Na} [Na^+]_i + p_{Cl} [Cl^-]_o} \right)$$

E_m is the resting membrane potential in volts, R, T and F are identical to those in Nernst equation, p_x is the permeability coefficient for ion X, and $[X]_e$ and $[X]i$ are the concentration of ion X in the extracellular and intracellular compartments respectively. The Goldman-Hodgkin-Katz equation assumes that ionic species contributing to the equilibrium potential are monovalent and do not interact among themselves. Thus, divalent ions such as Ca^{2+} are not included. The typical concentrations of the ionic species relevant to the resting membrane potential are shown Table 2 [Hammond01]:

The mechanism by which the resting membrane potential is established relies on the selective permeability of the neuronal plasma membrane. At rest, the plasma membrane is minimally permeable to Na^+ and Cl^- but highly permeable to K^+, that is, most of the K^+ channels are open. As a consequence, movement of K^+ occurs down its concentration gradient from the intracellular to the extracellular space while Na^+ and Cl^- move in the opposite direction at a slower rate. The intracellular and extracellular concentrations of Na^+ and K^+ are maintained through the activity of the Na^+-K^+ ATPase pump as previously described. It moves 2 K^+ ions into the neuron for every 3 Na^+ ions it removes from the neuron as shown in Figure 4. Less is known about the maintenance of Cl^- concentrations across the plasma membrane. It appears that a chloride pump could be functioning in a similar manner as the Na/K-ATPase pump [Matthews98].

3.3   The Generation and Propagation of an Action Potential

An action potential or nerve impulse is a rapid and transient depolarization of the neuronal plasma membrane. The action potential is initiated by some external stimulus, such as an impulse transmitted from another neuron. The stimulus causes an initial depolarization, which, upon reaching a threshold, triggers the action potential. Thus, the action potential is an all-or-none event; it does not occur unless a stimulus is sufficiently strong to reach the threshold level, but once the threshold is reached, the action potential is generated with an amplitude and form that are independent of the strength of the stimulus. In most neurons, the threshold level is around 10 to 20 mV above the resting membrane potential. An action potential is typically divided into three phases as shown in Figure 5:

- Depolarization
- Repolarization
- Hyperpolarization

Depolarization refers to a reduction in the membrane potential, that is, the potential attains a more positive value. It occurs rapidly once the threshold level is reached. Depolarization results from the opening of voltage-gated Na^+ channels, allowing the influx of Na^+ ions into the neuron and causing the intracellular space to be positively charged with respect to the extracellular space. Once the Na^+ channels have opened, their closure or inactivation occurs rapidly, causing depolarization to be short-lived.

Upon reaching its peak (when depolarization is maximally positive), the action potential undergoes a phase of repolarization. That is, the membrane potential becomes less positive and tends towards its equilibrium voltage. Repolarization is due in part to the inactivation of Na^+

channels as described above as well as the delayed opening of K^+ channels, resulting in the efflux of K^+. The overall effect is that the intracellular space becomes less positively charged and the membrane potential returns to its resting voltage. Unlike Na^+ channels, K^+ channels are not inactivated upon depolarization; rather they remain open until the membrane potential returns to its resting state.

As repolarization progresses, the membrane potential transiently undershoots its resting value, an event known as hyperpolarization. At this point the membrane's permeability to Na^+ has returned to that of the equilibrium potential while the permeability to K^+ is still above its resting level. As a consequence, the efflux of K^+ remains relatively high, causing the charge in the intercellular space, and hence, the membrane potential, to be more negative than what it is at equilibrium. As the K^+ channels close in response to repolarization, the membrane potential returns to its resting state.

From the moment an action potential starts until the time when the Na^+ channels begin to recover from inactivation, the membrane is in the *absolute refractory period* during which any stimulus, regardless of strength, cannot trigger a second action potential. This period is followed by the *relative refractory period* during which the neuronal membrane progressively returns to its resting state. An action potential may be triggered in this period, but requires a stimulus that is stronger than normal as the neuron is in a hyperpolarized state.

An action potential is generated at the initial segment of an axon, that is, the part of the axon attached to the soma. Once initiated, the action potential propagates itself along the axon. That is, the action potential creates a current that depolarizes the neighboring segment of the axon, which in turn, causes the depolarization of the subsequent neighboring segment. Although the depolarizing current spreads in both directions along the axon, the propagation of the action potential is unidirectional. This is because the segment of the axon that the action potential had just traversed is in its refractory period, and thus, cannot generate a second action potential. For a non-myelinated axon, an action potential is propagated along each point of the axon. In contrast, an action potential propagates more rapidly from one node of Ranvier to the next in a myelinated axon, a phenomenon known as *saltatory propagation*.

3.4   External Recording of Action Potentials

When an action potential propagates along an axon or dendrite, local circuit currents are generated. The intracellular and extracellular longitudinal currents are diphasic, that is, they initially travel forward and then in the reverse direction. These currents are recorded by surface electrodes attached to an oscilloscope. As shown in Figure 6, as an action potential moves along the axon from left to right, the accompanying intracellular current is registered as the positive phase of the oscilloscope waveform. The subsequent current in the opposite direction results in the negative phase of the waveform. If a segment of the axon between the recording electrodes is damaged, the action potential cannot reach the second electrode, thus, resulting in a monophasic waveform (Figure 7).

Spinal cord white matter comprises axons of multiple neurons. When a segment of white matter is stimulated, action potentials are generated simultaneously in various axons. The summation of these action potentials is an electrical response known as the *compound action potential* (CAP), which is used as an experimental indicator of axonal function. Although the action potential of each individual axon has an all-or-none characteristic as previously described, the compound action potential is graded and not all-or-none. That is, the maximum amplitude of the compound action potential increases with the intensity of the stimulus. The graded response is the result of a larger number of axons being activated as the stimulus intensity increases. Thus, with more axons being activated, the summation of external currents generated these axons produces a compound action potential of larger amplitude [Sperelakis01].

4.   Studies on the Histological and Physiological Effects of Spinal Cord Injury

The following is a review of various publications on experimental models evaluating the effects of SCI. These models involved the use of animal subjects in which SCI was experimentally induced. The damaged region of the spinal cord was assessed via microscopy, electrical recording and/or biochemical tests at various time periods after the injury. This review compares the models on the basis of the methods used to induce SCI and those for data collection as well as data itself. Some of the studies involved functional assessment, such as, the degree of limb paralysis and its recovery; however, this review focuses largely on data relating to microscopy, electrical conduction and biochemistry.

4.1   Experimental Methods for Inducing SCI

The papers reviewed showed a variety of methods for inducing SCI as described below. These methods were applied either in-vivo or in-vitro depending on the purpose of each study. For instance, an in-vivo method was applied if the study requires the assessment of motor dysfunction. The animals used in these studies were mainly adult rodents, namely, rats, mice and guinea pigs. A couple of studies were carried out on adult dogs [Stokes83] and cats [Blight83, Blight86]. In all studies, the methodology for inducing SCI was described to some extent; however, no details were provided on the dimensions of the spinal cord segments that were traumatized.

4.1.1   *Weight-Drop Method*

Since this method was reported in 1911 by Allen [Allen11], it has been widely used for in-vivo studies. It involved the immobilization of an anesthetized animal in a prone position. Laminectomy was performed on the thoracic vertebral column to expose the spinal cord. The dura mater, which is the tough fibrous membrane covering the spinal cord was kept intact. A weight was then dropped from a height onto the exposed dura, causing injury to the spinal cord beneath. To obtain a gradation of applied force, the height from which the weight was dropped was increased in steps [Nobel85, Wrathall85]. There is no apparent standardization in the application of this method among researchers. For instance, studies by Chesler, Happel and

Rosenberg used a single 10-gram weight but dropped it from 5, 30 and 2.5 cm respectively [Chesler91, Happel81, Rosenberg99, Rosenberg01]. In contrast, the studies by Blight and Stokes, performed on cats and dogs respectively, used a 20-gram weight dropped from a height of 20 cm [Blight83, Stokes83]. No details were provided with regards to the duration of compression. Differences are also noted in the design of the weight-drop device; Soblosky et al. employed a variant of Allen's device, using a serological pipette, which served as a housing for a Teflon ball attached to the upper end of a vertical metal compression rod. To induce SCI of different severity, a 10.5-gram weight was dropped from varying heights onto the Teflon ball [Soblosky01].

4.1.2   *Weight-Placement Method*

This is an in-vivo method used repeatedly by researchers at the Uppsala University Hospital in Sweden [Farooque00, LiGL96, LiGL00]. As in the weight-drop method, laminectomy was performed on the thoracic verterbral column, leaving the dura intact. The compression device consists of a 2 by 1 mm rectangular plastic plate attached to the bottom of a vertical 4 cm metal rod. The upper end of the rod was attached to a round plastic platform on which different weights are placed. A steel clamp around the rod was gently released to allow the gradual descend of the compression plate onto the spinal cord. The study did not explicitly state whether the compression plate was in contact with the dura before the rod was released, however, a diagram of the model seems to indicate that the plate was held slightly above dura prior to compression. SCI was induced with weights of 2, 5 and 10 grams per mm^2 sustained for a period of 5 minutes. An earlier study involving the same author appears to have used a similar procedure but with different weights, namely 9, 35 and 50 grams [LiGL96].

4.1.3   *Distance-Graded Method*

In this method, the amount of cord compression measured not in terms of the applied weight but in terms of the distance moved by the compression surface onto the cord [Shi96, Shi99]. It was carried out as an in-vitro method in Shi's model and applied to strips of white matter dissected from the spinal cord. Since the purpose of Shi's model was to evaluate the post-injury conduction properties of spinal cord axons, there was no apparent need for compression to be applied to an intact segment of the spinal cord. A strip of white matter was secured in a double sucrose gap recording chamber, containing three separate wells arranged in a row. The white matter strip stretched across the wells of which the ones at the two ends contained isotonic potassium chloride while the central well contained an isotonic sucrose solution. The segment of the white matter in the central well laid on a Plexiglas stage and was compressed from above by a Plexiglas rod over a 2.5 by 7 mm area. The movement of the compression rod was maintained at a constant speed by a stepper motor. Although both studies [Shi96, Shi99] are largely similar in the induction of SCI, there appear to be some differences. In the former, the compression rod was advanced at 24 microns per second and removed 15 seconds after complete failure of the compound action potential (CAP); in the latter, the compression rod was advanced at 25 microns per second until a target CAP amplitude was reached and removed without indication of a 15 second delay.

4.1.4 *Clip Method*

Some of the models reported using some form of a clip to induce SCI [Agrawal96, Agrawal97, Fehlings95, Li99, Li00, Nashmi01, Shi97]. Most were specified as an aneurysm clip or a modified aneurysm clip, presumably referring to the metallic vascular clips commonly used for surgical occlusion of cerebral aneurysms. There exists a wide variety of aneurysm clips with different shapes and sizes, for instance, clip blades may be straight, curved or angled [Louw01]. The studies, however, provided no information on the type of clips that were used or how they were modified. The amount of compression applied to the spinal cord was only briefly described; for instance "a 2 g force for 15 s" [Agrawal96, Agrawal97, Fehlings95] or "a 23-g clip injury … for 1 min"[Nashmi01]. Furthermore, no details were specified as to whether the clips were applied in contact with the dorsal, ventral or lateral surfaces of the spinal cord. Shi et al. [Shi97] described a similar method using a tool constructed from a watchmaker's forceps. As the study involved the evaluation of chronic response to SCI, the tool was applied in-vivo on either side of the spinal cord and used to compress the a 5 mm long region of the cord to a thickness of 1.2 mm for 15 seconds.

4.2   Effects of Mechanical Stress on the Spinal Cord

Studies appear to indicate the effects of mechanical compression of the spinal cord occur in two phases [Fehlings95, Agrawal96, Rosenberg99]. The first phase, known as primary injury, includes the direct consequences of the mechanical injury. The second phase, known as secondary injury, occurs hours to days after the initial injury. It comprises trauma-induced physiological and biochemical effects such as, reduced oxygen perfusion and inflammatory cellular reactions. SCI has also been described as "acute" "subacute" or "chronic" although there is no universal agreement on the exact post-injury periods that these terms refer to. Shi et al. defined the term "acute" to encompass immediate consequences of SCI occurring within the first few hours of injury. These effects include the initial mechanical disruption and subsequence changes in membrane permeability that causes shifts in intracellular and extracellular concentrations of bioactive substances. "Subacute" was defined as the period between 24 hours to 3-4 weeks after injury during which intensive inflammatory reaction and tissue repair occurred. Following the "subacute" phase, the histopathology and functional aspects of the injury remains relatively stable; this period was referred to as "chronic". The models that were reviewed focused on various aspects of the SCI, that is, primary, secondary, acute or chronic, depending on their individual objectives. In general, the consequences of spinal cord compression analyzed by these models were categorized into histological, electrical and biochemical effects as described below. Although the functional aspect, such as the extent and recovery of limb paralysis was also analyzed in some of the models [Farooque00, Soblosky01, Wrathall85], it is not considered in this review.

4.2.1 *Histological Effects*

In the studies involving histological evaluation, sections of the spinal cord were examined through a light or electron microscope. Depending on the objectives of each study, spinal cord

specimens were prepared within hours of the injury for assessment of acute histological changes and/or weeks later for chronic changes. Some provided only a general description of the histopathology [Farooque00, Fehlings95, LiGL00] while others attempted to quantify the extent of injury using various grading schemes [Farooque01, Nashmi01, Rosenburg99, Soblosky01]. In the study by Rosenberg, Teng and Wrathall [Rosenberg99], the extent of injury was graded on electron micrographs using the axonal injury index (AII). The histopathology of each axonal cross section was classified into four categories, namely myelin pathology, axoplasmic pathology, periaxonal space and necrotic axoplasm as shown in Table 3. Points were allocated to each category according to the presence of one or more pathological changes. For instance, myelin pathology was defined as "unwinding of the myelin lamellae that can be either slight or severe unraveling, appearing as whorls of membranous matter, abnormal spaces in between the lamellae, hypermyelination or hypomyelination, and fragmentation of the myelin sheath". Summing the points allocated to all the categories and dividing the result by the total number of axons in the micrograph produced the AII for that animal. Without calculating the AII, the point system itself provides a means of quantifying the extent of injury for each individual axon. However, there remains a degree of subjectivity based on the visual judgment of the person evaluating the micrograph.

Another method described by Farooque et al. was based on computerized microscopy image analysis of stained spinal cord sections 14 days post-injury [Farooque01]. The sections were stained with Luxol fast blue-cresyl violet as well as immunostained with antibodies against microtubule-associated protein 2 (MAP2), glial fibrillary acidic protein (GFAP) and ionized calcium binding adapter molecule 1 (iba1). As the stains were localized to different areas in the spinal cord, they were used to assess the extent of local damage. In specific, Luxol stained the myelinated axons in the white matter while MAP2, the neurons and dendrites in the gray matter. GFAP staining revealed strong immunoreactivity in astrocytic cells processes of the white matter and iba1 staining was confined to microglial cells, which are most commonly found in the white matter. The areas of the portions with different stains were determined through computerized image analysis. Luxol and MAP2 staining could probably be used to evaluate acute damage within hours of the applied compression since they do not appear to be dependent on degree of immunological response to the injury. In contrast, GFAP and iba1 staining appear to be affected respectively by astrocytic and microglial reactions to injury and, thus, may not be suitable for early assessment of tissue damage. Nonetheless, quantification of cord injury through image analysis has an advantage over the AII method in that it is not affected by subjective human visual assessment of the injury.

The study by Nashmi and Fehlings [Nashmi00] used another method of injury quantification. A CCD (charge coupled device) video camera captured microscopy images, which were analyzed quantitatively offline with the Image Pro Plus software. A protocol was designed to ensure a non-biased sampling of each image field. This involved a grid of ten equally spaced vertical lines overlaid and centered on each image field. Only the axons superimposed by the grid lines were analyzed for their diameter and myelination ration (MR). The latter was defined as the diameter of an axon and its myelin sheath divided by the axonal diameter. Thus, a completely demyelinated axon had a MR of one while a myelinated axon had a MR of greater than one. In addition, the number of axons per field was estimated by multiplying the cross-sectional area of the tissue section by the mean number of axons per field determined by the line sampling

technique and dividing the result by the area of the sampled field. Since the extent of axonal degeneration varies as a function of the post-injury duration, estimating the number of axons per field is appropriate only after the commencement of axonal loss, which is more evident in the subacute or chronic SCI than in the acute phase.

In general, the epicenter of the injury revealed swollen axonal profiles as early histological evidence of compression trauma [Fehlings95, Lopachin99, Rosenberg99]. The severity of these pathological changes corresponded to the extent of compression. In specific, the changes include a decrease in myelin thickness, splitting or unwinding of the myelin sheath, fluid accumulation between the axon and the myelin sheath (periaxonal swelling) and compaction of the axonal cytoplasm. Periaxonal swelling is revealed by enlarged spaces between the axolemma and inner lamella of the myelin sheath. These spaces are occasionally seen in uninjured axons but are less than 25% of the intramyelin area [Rosenberg99]. Within the axoplasm, the effects of trauma appeared in the form of mitochondrial swelling, condensation or loss of neurofilaments and microtubules and the presence of vesiculation or vacuoles. Some axons were noted to consist entirely of flocculent substance, indicating the total destruction of cytoskeletal structures. These changes were noted as early as one hour after the injury.

In terms of chronic injury, there appears to be a wide variation in gross morphology of the lesion reported in different studies. This is not surprising considering the wide variations among these studies in terms of the types of animals used, the method of inducing SCI and the length of time between injury and histological analysis. The correlation between the cross-sectional area of the damaged cord or the extent of central cavitation and the force of impact is controversial. Noble and Wrathall noted that the total cross-sectional area of the damaged cords were inversely related to the height from which weights were dropped. This reduction in size was due to a loss in the constituents of the gray and white matter. The degree of central cavitation was also general reported to enlarge with increasing drop height [Noble85]. These findings are consistent with the gelatin model constructed by Blight and Decrescito, in which a horizontal Silastic tube filled with gel was compressed from above. Movement of the gel made visible by ink tracks showed that the center of the tube was subjected to the greatest displacement. Thus, structures at the center of the impact site in the spinal cord are likely to suffer the greatest strain. However, Blight and Decrescito cautioned that the overall cross-sectional area of the lesion or central cavitation does not necessarily correlate to the extent of neural damage [Blight86]; lesions with a similar number of central axons were found to have different cross-sectional areas and degree of central cavitation.

A common feature appears to be the preservation of white matter that increases progressively towards the perimeter of the cord [Blight86, Nashmi01]. The axons in the outer rim of the cord subjected to the weight-drop method were rather evenly distributed around the circumference of the cord except for the zone of greatest destruction at dorsolateral regions [Blight86]. The reduction in number of axons was found to vary somewhat exponentially with depth and linearly in the outer rim of the cord. It was postulated that the loss of axons was due primarily to the initial mechanical strain at the time of impact. The centrifugal pattern of axonal distribution could be explained by the longitudinal displacement of the structures in the center of the cord, indicating the "boundary layer" effect of compression on viscoelastic material bounded within the meninges, as illustrated by the gelatin model described above [Blight86]. In addition, axonal

pathology was characterized by abnormally thin myelin sheaths and empty myelin profiles indicating degenerated axons. The extent of demyelination varied with the intensity of injury and overall axonal survival [Blight86]. The thin myelin sheaths may have been the result of one or more factors, namely, partial demyelination, complete demyelination and subsequent remyelination with abnormally thin myelin sheaths or stretching of the myelin sheath by axonal swelling. Blight and Decrescito also reported that in lesions with extensive survival of the pia, surviving axons were concentrated around the pial surface whereas the opposite was true with significant pial destruction. In line with this finding, Rosenberg and Wrathall noted a high density of axons remaining in a rim around the ventral pia within a confluent astrocytic matrix. Areas without confluent glial matrix were reported to have isolated astrocytes, oligodendrocytes and inflammatory cells [Rosenberg01].

4.2.2 *Electrical Effects*

The evaluation of electrical conduction through traumatized spinal cord tissue was base on the measurement of monophasic compound action potential (CAP) responses to electrical stimuli before injury and at various intervals after injury. Some studies analyzed the CAP for acutely injured axons, that is, within hours of the applied compression [Agrawal96, Agrawal97, Shi96, Shi99, Li99, Li00, Lopachin99] while other studies were concerned about the CAP response weeks after the injury [Blight83, Nashmi01]. Shi and Blight [Shi96] identified three types of conduction block caused by compression: an immediate and spontaneously reversible block, possibly due to ionic deregulation resulting from a transient increase in membrane permeability; a second type of block that was irreversible within one to two hours of recording, possibly due to complete axonemmal disruption; and a third type of block, apparently reversible with the potassium channel block, 4-aminopyrimidine, may be due to myelin sheath disruption.

In general, the amplitude of a CAP measured within hours of the injury decreased with increasing degree of focal compression [Shi96, Shi99, Lopachin99]. Using distance-graded compression and sucrose gap recording, Shi et al. noted that the potential was almost completely abolished at 80% compression. The effect on the latency of a CAP, that is, the duration between the application of a stimulus and the start of a CAP appears to be controversial. Two studies reported that cord compression prolonged CAP latency [Fehlings95, Shi96], but Lopachin et al. [Lopachin99] noted no significant alternation in CAP latency. As a result of the grossly unaltered form and latency of the CAP, Lopachin et al. concluded that the decrease in CAP amplitude was due to a reduction in the total number of axons contributing to the CAP instead of changes in the temporal distribution of the action potentials from these axons [Lopachin99]. Shi and Blight explained that an increase in latency is most likely due to damage to myelin sheaths, causing increased internodal capacitance and action potential transit time. In the study by Shi and Blight, the refractory period of the CAP showed only a small change following injury. The absolute refractory period was significantly increased after injury [Fehlings95, Shi96]; however no change was found in the relative refractory period [Shi96]. In addition, the temperature of the tissue was shown to affect electrical conduction during the acute phase of injury. The amplitude, duration and conduction delay of the CAP decreased when temperature was increased from 25°C to 37°C [Shi96]. Recovery of the membrane potential to the resting level in traumatized tissue was found to vary with temperature [Shi00]. Recovery of membrane potential for cords

transected at 37°C was about 97% at one hour post-injury whereas cords transected at 25°C showed not significant recovery of membrane potential in the same time. Relief of the compression within seconds of its commencement resulted in the progressive recovery of both the amplitude and latency of the CAP. However, the recovery was partial, stabilizing within minutes and remained so for one to four hours post-injury [Fehlings95, Shi96, Shi99, Lopachin99].

For studies that evaluated the electrical characteristics of chronically damaged spinal cord tissue, recordings were usually taken around 4 to 8 weeks after injury. Axons with chronic injury were found to have markedly reduced CAP amplitude compared to non-injured axons as well as significantly reduced conduction velocity [Nashmi01, Honmou96]. Nashmi and Fehlings also noted that a greater stimulus was needed not only to elicit a minimal response from the damaged tissue but also to stimulate at least half of the conducting axons in the damaged tissue. These findings suggest that chronically damaged axons are significantly less excitable compared to normal axons, which is a possible factor causing the reduction in CAP amplitude. An increase in refractory period and a decrease in conduction velocity were also reported for injured axons [Nashmi01, Honmou96]; however, no details were given regarding the absolute and relative refractory periods. Concerning the effects of temperature change, an increase in tissue temperature from room levels (23-25°C) to physiological levels (36-37°C) resulted in an increase in CAP amplitude and a reduction in the refractory period, a finding that was consistent with acutely injured tissue [Shi96]. Blight, however, reported that electrical conduction failed in only 7% of the axons in uninjured spinal cord tissue at temperatures below physiological levels but in 93% of chronically injured tissue, indicating the presence of conduction blocking factors other than temperature change.

In both acute and chronic spinal cord injury, the changes in electrical conduction may be caused by physical abnormalities of the axons and/or myelin sheaths as well as derangement in ionic concentrations. The latter explained in the next section on biochemical effects. Among the physical changes, the reduction in myelin sheath thickness is a likely factor that contributes to axonal dysfunction [Nashmi01]. Myelin plays a vital role in reducing axonal membrane capacitance. This results in a more rapidly changing membrane potential, which results in an increase in axonal conduction velocity. A reduction in capacitance also increases the safety of axonal conduction by reducing the total current needed to raise the membrane potential to the threshold level. Furthermore, the myelin sheath also produces more rapid repolarization of the membrane potential, allowing a more frequent propagation of action potentials. Thus, thinning of the myelin sheath explains the decreased conduction velocity and increased refractory period in chronically injured axons.

Another suggested mechanism of electrical dysfunction in chronic SCI is impedance mismatch [Nashmi01]. The swollen axonal profiles and overall increase in median axonal diameter in axons with chronic damage provide a low safety for axonal propagation. That is, there is a lower probability of successful propagation of action potentials from a region with a smaller diameter to one with a larger diameter. This is because the smaller current and higher resistance within the region with the smaller diameter may not be sufficient to raise the membrane potential to the threshold level in the region with the larger diameter. Impedance mismatch may also occur in the transition from a region with normal myelination to an unmyelinated or thinly myelinated region

of an axon. This is due to a decrease in resistance to transmembrane current flow in the latter. Impedance mismatch is a possible factor contributing to electrical changes in the acute phase of SCI in which swollen axonal profiles were also reported.

4.2.3 *Biochemical Effects*

A variety of elemental species were evaluated in the four studies [Chesler91, Happel81, Lopachin99, Stokes83]. Chesler et al. and Stokes et al. used ion-selective microelectrodes to evaluate changes in the concentration of K^+ and Ca^{2+} respectively. According to Stokes, K^+-selective electrodes have selectivity over Na^+ but they had a tendency to lose their selectivity rapidly over several hours of tissue monitoring. K^+ responses were also found to vary widely among different animals. In contrast, Ca^{2+}-selective electrodes were reported to be superior in stability and ionic selectivity. Other methods of biochemical analysis included the use of atomic absorption spectroscopy and electron probe x-ray microanalysis (EPMA) to measure water content and various elemental concentrations [Happel81, Lopachin99]. Among the studies reviewed, only Lopachin et al. used a model of graded focal injury.

The studies show that acute SCI is characterized by a derangement in axonal elemental concentrations and water content. Within minutes of the compression, the extracellular space at the site of injury revealed an increase in K^+ concentration [Chesler91]. There is also a decrease in extracellular Ca^{2+} concentration, which recovers gradually until 1.5 hours after injury. This is followed by an abrupt increase in mean Ca^{2+} activity [Stokes83]. However, the extracellular Ca^{2+} concentration remained lower than that of uninjured tissue 3 hours after injury. The corresponding biochemical changes in the damaged axons are characterized by an increase in Na^+, Cl^-, Ca^{2+} concentrations and a decrease in water content as well as K^+ and Mg^{2+} concentrations [Happel81, Lopachin99]. The use of voltage-gated K^+ channel blocker, 4-aminopyrimidine, improved electrical conduction in acutely injured axons, indicating that the shift in K^+ concentrations is mediated by K^+ channels [Fehlings97, Shi97]. Research evidence based on the use of the Na^+ channel blocker, tetrodotoxin, suggests that the increase in intracellular Na^+ concentration is mediated by voltage-gated Na^+ channels [Rosenberg99, Yang97]. Focal administration of tetrodotoxin into the injury site within minutes after compression injury significantly reduced tissue loss at the injury site as well as functional deficits. This finding noted on microscopy within the first day and at eight weeks after injury, supports the role of Na^+ channels in acute neurotoxicity following SCI. The Na^+-H^+ antiport, which exports Na^+ while importing H^+, has also been implicated in the mechanism of secondary injury. Inhibition of this antiport conferred significant neuroprotection acutely damaged cord tissue, suggesting the possibility of intracellular acidosis caused by failure of the antiport [Agrawal96]. Blockade of the Na^+-K^+ ATPase pump, which extrudes Na^+, resulted in poorer CAP recovery in acute SCI, pointing to a reduction in Na^+ efflux due to trauma-induced dysfunction of the Na^+-K^+ ATPase pump [Agrawal96]. The reverse Na^+-Ca^{2+} antiport, which simultaneously imports Ca^{2+} ions and exports Na^+ ions may also be a contributing mechanism. Although the simultaneous elevation of intra-axonal Na^+ and Ca^{2+} concentrations suggests the role of the reverse Na^+-Ca^{2+} antiport, pharmacological inhibition of this antiport by Agrawal and Fehlings revealed no significant improvement of CAP amplitude in the acute phase of injury. However, the study by Li et al. performed at physiological temperature showed otherwise,

suggesting that the findings by Agrawal and Fehlings may have been caused by lower temperatures [Li00]. With graded focal injury, elemental composition of axons at the epicenter of the injury was noted to recover to near control values by one hour after moderate compression (gap width of 250μm) whereas severe compression (gap width of 700 μm) did not reveal significant elemental recovery [Lopachin99].

Acute SCI involves a component of glutamate-mediated damage to white matter, the mechanism of which appears to involve the overactivation of ionotropic glutamate receptors. These receptors are subdivided into three categories, namely, NMDA (N-methyl-D-aspartate), AMPA (alpha-amino-3-hydroxy-5-methyl-4-isoxazolepropionic acid) and kainate receptors. NMDA receptors are permeable to Na^+, K^+ and Ca^{2+} while AMPA and kainate receptors, which were previously thought to be permeable only to monovalent ions, have certain subtypes that are permeable to Ca^{2+} [Gilbertson91, Iino90, Pelligrini97]. Although NMDA receptors have been implicated in non-traumatic neuronal injury [Goldberg93], their role in traumatic injury is controversial. Using in-vitro trauma to white matter, Agrawal and Fehlings reported no changes in CAP amplitude with NMDA receptor agonist or antagonist [Agrawal97]. In contrast, the activation of AMPA and kainate receptors has been shown to attenuate peak CAP amplitude [LiS00] while their blockade improved the recovery of CAP amplitude after compression injury [Agrawal97]. Another proposed glutamatergic mechanism is the reverse Na^+-dependent glutamate transport. Li et al. demonstrated the release of endogenous glutamate via the reversal of Na^+-dependent glutamate transport in acutely injured white matter [Li99]. The uncontrolled efflux of glutamate into the periaxonal space could activate AMPA receptors, resulting in damage to myelin and other structures.

As for biochemical changes after the acute phase of SCI, K^+ channels appear to play an important role in chronic SCI as revealed by the improvement in electrical conduction following the application of 4-aminopyrimidine [Shi97, ShiB97]. However, lower concentrations of 4-aminopyrimidine were required to elicit a significant response than in the acute phase of injury. Using Western blotting and immunofluorescence microscopy, Nashmi et al. reported an increased expression of Kv1.1 and Kv1.2 K^+ channel proteins in chronic SCI. These proteins showed a more dispersed pattern along injured axons as opposed to the paired juxtaparanodal localization in normal axons [Nashmi00]. Intracellular Ca^{2+} remained elevated up to one week post-injury based on a non-graded weight-drop method [Chesler91]. As in acute SCI, AMPA and kainate receptors may play an important role in chronic SCI; the antagonism of AMPA and kainate receptors 4 hours after compression injury reduced functional deficits 8 weeks after the injury [Wrathall97].

Elemental derangement clearly underlies electrical dysfunction in both acute and chronic SCI as shown by the studies relating the effect of ion channel blockers on CAPs. In acute SCI, there is a rapid and complete loss of transmembrane ionic gradients [Lopachin99]. Although the exact mechanism of elemental deregulation is unknown, mechanical shearing of the axolemma with increased membrane permeability is an implicated factor [Blight86]. Considering specific elemental species, the reduction and slow recovery of extracellular Ca^{2+} concentration [Stokes83] together with an increase in total Ca^{2+} in injured spinal tissue are evidence of an immediate and continuing influx of Ca^{2+} into the intracellular space. Stokes et al. suggested that such a shift in Ca^{2+} concentration could result in a decrease in threshold voltage of the neuronal

membrane but did not elaborate how such an effect would influence CAPs. An accumulation of intracellular Ca^{2+} may also depress calcium-dependent conductance. As for chronic SCI, the activation of K^+ channels is implicated in axonal dysfunction as evident by the improvement in conduction with 4-aminopyrimidine. The lower concentrations of 4-aminopyrimidine required to induce a significant electrical response in the chronic phase indicates the incomplete process of repair resulting in partially myelinated axons [Shi97]. In addition, the increased expression and wider dispersion of Kv1.1 and Kv1.2 K^+ channel proteins point to an adaptive process in which an increase in K^+ channels results in shunting of the Na^+ current, causing reduced axonal excitability [Nashmi01].

Cellular Ca^{2+} overload may also indirectly cause electrical dysfunction by promoting cellular necrosis, which is evident in the subacute and chronic phases of SCI. Happel et al. suggested that certain Ca^{2+}-dependent phospholipases may be activated by the high intracellular concentration of Ca^{2+} and consequently produce lysolecithin, a myelinolytic compound. Likewise, certain proteinases, which are activated by Ca^{2+}, may cause enzymatic breakdown of proteins necessary for the structural stability of myelin. Cellular Ca^{2+} overload may also cause myelin damage via an excitotoxic mechanism, such as that involving AMPA and kainate and glutamate receptors [Agrawal97]. These Ca^{2+}-permeable receptors are an importance means of Ca^{2+} influx into neurons. It was suggested that damage to the myelin sheath occurred as a direct process but may also have been secondary to injury of parent oligodendrocytes [LiS00].

5.   Conclusion

A review of experimental animal studies on SCI was performed to analyze the methods of inducing compressive SCI as well as the histological, electrical and biochemical data. Four categories of cord compression techniques were identified, namely, dropping weights onto the cord, placing weights on the cord, distance-based compression and the application of aneurysm clips. The first two were largely in-vivo procedures in which the cord remains covered by the intact dura during compression while the last two were usually applied in-vitro to tissue dissected from the cord. The absence of standardization in the procedure of inducing experimental SCI introduces variability in the mechanics of the applied force. Notwithstanding these differences, the studies showed several common effects of mechanical trauma to the spinal cord. Early histological findings at the epicenter of injury included axoplasmic compaction, periaxonal swelling, decrease in myelin thickness and splitting or unwinding of the myelin sheath. In chronic SCI, there was loss of gray and white matter with surviving axons located largely at the rim of the damaged cord. This pattern of injury was attributed to the "boundary layer" properties of the cord as a bounded viscoelastic material. In terms of electrical conduction, the acute phase of SCI showed axonal function progressively degenerating with increasing severity of impact and partially improving after relief of compression. Poor electrical conduction was likewise found in chronic SCI. These changes may be explained by physical disruption to myelin sheaths as well as ionic deregulation. Electrical conduction was significantly affected by temperature changes, pointing to the importance of considering the variation in in-vivo and in-vitro experimental parameters. The latter was characterized by an efflux of K^+ into the extracellular space and an intraaxonal accumulation of Na^+ and Ca^{2+} in acute SCI. Intracellular Ca^{2+} concentration, which remained high in chronic SCI, has been implicated as a factor in secondary

damage of axons and myelin sheaths. Research evidence points to a number of membrane channels as part of the mechanism underlying elemental derangement, namely, voltage-gated K^+ and Na^+ channels, Na^+-H^+ antiports, Na^+-K^+ ATPase pumps, Na^+-Ca^{2+} antiports. In addition, the overactivation of ionotropic glutamate receptors of the NMDA, AMPA and kainate classes has been postulated as a means of damage to white matter.

References

Agrawal96   Agrawal S.K., Fehlings M.G. "Mechanisms of Secondary Injury to Spinal Cord Axons In Vitro: Role of Na^+, Na^+-K^+-ATPase, the Na^+-H^+ Exchanger, and the Na^+-Ca^{2+} Exchanger", *Journal of Neuroscience*, Vol. 16, No. 2, 1996, pp, 545-552.

Agrawal97   Agrawal S.K., Fehlings M.G. "Role of NMDA and Non-MNDA Ionotropic Glutamate Receptors in Traumatic Spinal Cord Axonal Injury", *Journal of Neuroscience*, Vol. 17, No. 3, 1997, 1055-1063.

Aidley96   Aidley D., Stanfield P. *Ion Channels: Molecules in Action.* Cambridge University Press, Cambridge, 1996.

Allen11   Allen A.R. "Surgery of Experimental Lesion of Spinal Cord Equivalent to Crush Injury of Fracture Dislocation of Spinal Column: a Preliminary Report", *Journal of the American Medical Association*, Vol. 57, pp. 878-880.

Atkinson01   Atkinson L., Merry G., "Advances in Neurotrauma in Australia 1970-2000", *World Journal of Surgery*, Vol. 25, 2001, 1224-1229.

Blight83   Blight A.R. "Axonal Physiology of Chronic Spinal Cord Injury in the Cat: Intracellular Recording In Vitro", *Neuroscience*, Vol. 10, No. 4, 1983, pp. 1471-1486.

Blight86   Blight A.R. Decrescito V., "Morphometric Analysis of Experimental Spinal Cord Injury in the Cat: The Relation of Injury Intensity to Survival of Myelinated Axons", *Neuroscience*, Vol. 19, 1986, pp. 321-341.

Celani01   Celani M. G. et al. " Spinal Cord Injury in Italy: A Multicenter Retrospective Study", *Archives of Physical Medicine and Rehabilitation*, Vol 82, May 2001, 589-596.

Chesler91   Chesler M. et al. "Elevation and Clearance of Extracellular K^+ Following Contusion of the Rat Spinal Cord", *Brain Research*, Vol. 556, 1991, pp. 71-77.

Cooper00   Cooper G.M. *The Cell: A Molecular Approach.* Sinauer Associates, Massachusetts, 2000.

Farooque00   Farooque M. "Spinal Cord Compression Injury in the Mouse: Presentation of a Model Including Assessment of Motor Dysfunction" *Acta Neuropathlogica*, Vol. 100, 2000, pp. 13-22.

Farooque01   Farooque M., Isaksson J., Olsson Y. "White Matter Preservation After Spinal Cord Injury in ICAM-1/P-selectin-deficient Mice", *Acta Neuropathologica* (Online), 25 July 2001, DOI 10.1007/s004010000307.

Fehlings95   Fehlings M.G., Nashmi R. "Assessment of Axonal Dysfunction in an In-vitro Model of Acute Compressive Injury to Adult Rat Spinal Cord Axons", *Brain Research*, Vol. 667, 1995, pp. 291-299.

Fehlings96   Fehlings M.G., Nashmi R. "Changes in Pharmacological Sensitivity of the Spinal Cord to Potassium Channel Blockers Following Acute Spinal Cord Injury", *Brain Research*, Vol. 736, 1996, pp. 135-145.

Gilbertson91   Gilbertson T.A., Scobey R., Wilson M., "Permeation of Calcium Ions Through Non-NMDA Glutamate Channels in Retinal Bipolar Cells", *Science*, Vol. 251, 1991, pp. 1613-1615.

Goldberg93   Goldberg M.P., Choi D.W., "Combined Oxygen and Glucose Deprivation in Cortical Cell Culture: Calcium-dependent and Calcium-independent Mechanisms of Neuronal Injury", *Journal of Neuroscience*, Vol. 13, 1993, pp. 3510-3524.

Hammond01   Hammond C. *Cellular and Molecular Neurobiology*. Academic Press, London, 2001.

Happel81   Happel R.D. et al. "Ca^{2+} Accumulation in Experimental Spinal Cord Trauma", *Brain Research*, Vol. 211, 1981, pp. 476-479.

Honmou96   Honmou O. et al. "Restoration of Normal Conduction Properties in Demyelinated Spinal Cord Axons in the Adult Rat by Transplantation of Exogenous Schwann Cells", *Journal of Neuroscience*, Vol. 16, No. 10, 1996, pp. 3199-3208.

Iino90   Iino M., Ozawa S., Tsuzuki K. " Permeation of Calcium Through Excitatory Amino Acid Receptor Channels in Cultured Rat Hippocampal Neurones", *Journal of Physiology*, Vol. 424, 1990, pp. 154-165.

LiGL96   Li G.L. et al. "Increasing Expression of Growth-associated Protein 43 Immunoreactivity in Axons Following Compression Trauma to Rat Spinal Cord", *Acta Neuropathlogica*, Vol. 92, 1996, pp. 19-26.

LiGL00   Li G.L. et al. "Changes of Fas and Fas Ligand Immunoreactivity After

Compression Trauma to Rat Spinal Cord", *Acta Neuropathologica*, Vol. 100, 2000, pp. 75-81.

Li99   Li S. et al. "Novel Injury Mechanism in Anoxia and Trauma of Spinal Cord White Matter: Glutamate Release via Reverse Na^+-dependent Glutamate Transport", *Journal of Neuroscience*, Vol. 19, 1999, RC16, pp. 1-9.

Li00   Li S. et al. "Important Role of Reverse Na^+-Ca^{2+} Exchange in Spinal Cord White Matter Injury at Physiological Temperature", *Journal of Neurophysiology*, Vol. 84 No. 2 Aug 2000, pp. 1116-1119.

LiS00   Li S., Stys P.K. "Mechanisms of Ionotropic Glutamate Receptor-Mediated Excitotoxicity in Isolated Spinal Cord White Matter", *Journal of Neuroscience*, Vol. 20, No. 3, pp.1190-1198.

Lopachin99   LoPachin R.M. et al. "Experimental Spinal Cord Injury: Spatiotemporal Characterization of Elemental Concentrations and Water Contents in Axons and Neuroglia", *Journal of Neurophysiology* Vol. 82, No. 5, Nov 1999, pp. 2143-2153

Louw01   Louw D. F., Asfora W.T., Sutherland G.R. "A Brief History of Aneurysm Clips", *Neurosurgical Focus*, Vol. 11, No. 2, Article 4, 2001.

Matthews98   Matthews G. *Cellular Physiology of Nerve and Muscle*. Blackwell Science, Massachusetts, 1998.

McDonald99   J. W. McDonald, "Repairing the damaged spinal cord", *Scientific American*, September, 1999, pp. 65 – 73.

McKinley99   McKinley W.O. et al. "Long-term Medical Complications After Traumatic Spinal Cord Injury: A Regional Model Systems Analysis", *Archives of Physical Medicine and Rehabilitation*, Vol. 80, Nov 1999, 1402-1410.

Nashmi00   Nashmi R., Jones O.T., Fehlings M.G. "Abnormal Axonal Physiology is Associated with Altered Expression and Distribution of Kv1.1 and Kv1.2 K^+ Channels After Chronic Spinal Cord Injury", *European Journal of Neuroscience*, Vol. 12, No. 2, 2000, pp. 491 (abstract).

Nashmi01   Nashmi R., Fehlings M.G. "Changes in Axonal Physiology After Chronic Compression Injury of the Rate Thoracic Spinal Cord" *Neuroscience*, Vol. 104, No. 1, pp. 235-251, 2001.

Noble85   Noble L.J., Wrathall J.R. "Spinal Cord Contusion in the Rat: Morphometric Analyses of Alterations in the Spinal Cord", *Experimental Neurology*, Vol. 88, 1985, pp. 135-149.

Pellegrini97 Pelligrini-Giampietro D. E. et al., "The GluR2 (GluR-B) Hypothesis: Ca^{2+}-permeable AMPA Receptors in Neurological Disorders", *Trends in Neuroscience*, Vol. 20, No. 10, 1997, pp. 464-470.

Nobunaga99 Nobunaga A.I. et al. "Recent Demographic and Injury Trends in People Served by the Model Spinal Cord Injury Care Systems", *Archives of Physical Medicine and Rehabilitation*, Vol. 80, Nov 1999, pp. 1372-1382.

Rosenberg99 Rosenberg L.J., Teng Y.D., Wrathall J.R. "Effects of the Sodium Channel Blocker Tetrodotoxin on Acute White Matter Pathology After Experimental Contusive Spinal Cord Injury", *Journal of Neuroscience*, Jul 15, 1999, 19(14), 6122-6133

Rosenberg01 Rosenberg L.J., Wrathall J.R. "Time Course Studies on the Effectiveness of Tetrodotoxin in Reducing the Consequences of Spinal Cord Contusion", *Journal of Neuroscience Research*, Vol. 66, 2001, pp. 191-202.

Shi96 Shi R., and Blight A.R., "Compression injury of mammalian spinal cord in vitro and the dynamics of action potential conduction failure", *Journal of Neurophysiology*, Vol. 76, 1996, pp. 1572 – 1580.

Shi97 Shi R., Kelly T.M., Blight A.R. "Conduction Block in Acute and Chronic Spinal Cord Injury. Different Dose-Response Characteristics for Reversal by 4-Aminopyrimidine", *Experimental Neurology*, Vol. 148, 1997, pp. 495-501.

Shi99 Shi R., Borgens R.B. "Acute Repair of Crushed Guinea Pig Spinal Cord by Polyethylene Glycol", *Journal of Neurophysiology* Vol. 81, No. 5, May 1999, pp. 2406-2414

Shi00 Shi R., Pryor J.D. "Temperature Dependence of Membrane Sealing Following Transection in Mammalian Spinal Cord Axons", *Neuroscience*, Vol. 98, No. 1, 2000, pp. 157-166.

ShiB97 Shi R., Blight A.R., "Differential Effects of Low and High Concentrations of 4-Aminopyrimidine on Axonal Conduction in Normal and Injured Spinal Cord", *Neuroscience*, Vol. 77, No. 2, 1997, pp. 553-562.

Soblosky01 Soblosky J.S., Song J.H., Dinh D.H. "Graded Unilateral Cervical Spinal Cord Injury in the Rat: Evaluation of Forelimb Recovery and Histological Effects", *Behavioural Brain Research*, Vol. 119, 2001, pp. 1-13.

Sperelakis01 Sperelakis N. *Cell Physiology Sourcebook: A Molecular Approach.* Academic Press, California, 2001.

Stokes83 Stokes B.T. et al. "Extracellular Calcium Activity in the Injured Spinal Cord", *Experimental Neurology*, Vol. 80, 1983, pp. 561-572.

Wrathall85   Wrathall J.R. et al. "Spinal Cord Contusion in the Rat: Production of Graded, Reproducible, Injury Groups", *Experimental Neurology*, Vol. 88, 1985, pp. 108-122.

Wrathall97   Wrathall J.R., Yang D.T., Marriott R. "Delayed Antagonism of AMPA/Kainate Receptors Reduces Long-Term Functional Deficits Resulting from Spinal Cord Trauma", *Experimental Neurology*, Vol. 145, 1997, pp. 565-573.

Yang97   Yang D.T., Wrathall J.R. "Local Blockade of Sodium Channels by Tetrodotoxin Ameliorates Tissue Loss and Long-Term Functional Deficits Resulting from Experimental Spinal Cord Injury", *Journal of Neuroscience*, Vol. 17, No. 11, 1997, pp. 4359-4366.

Table 1: Classification of ion channels

	Voltage-gated	**Ligand-gated**	**Mechanically-gated**
Stimulus	Change in membrane potential	Binding to intracellular or extracellular ligand	Mechanical
Examples	Na^+, K^+, Ca^{2+} channels	Ca^{2+}, G protein channels	Stretch-activated channels

Table 2: Concentrations of ionic species at equilibrium

Ion	Intracellular concentration	Extracellular concentration
Na^+	7	140
K^+	140	3
Cl^-	7	140

Table 3: Calculation of the Axonal Injury Index (AII)
(Adapted from Rosenberg99)

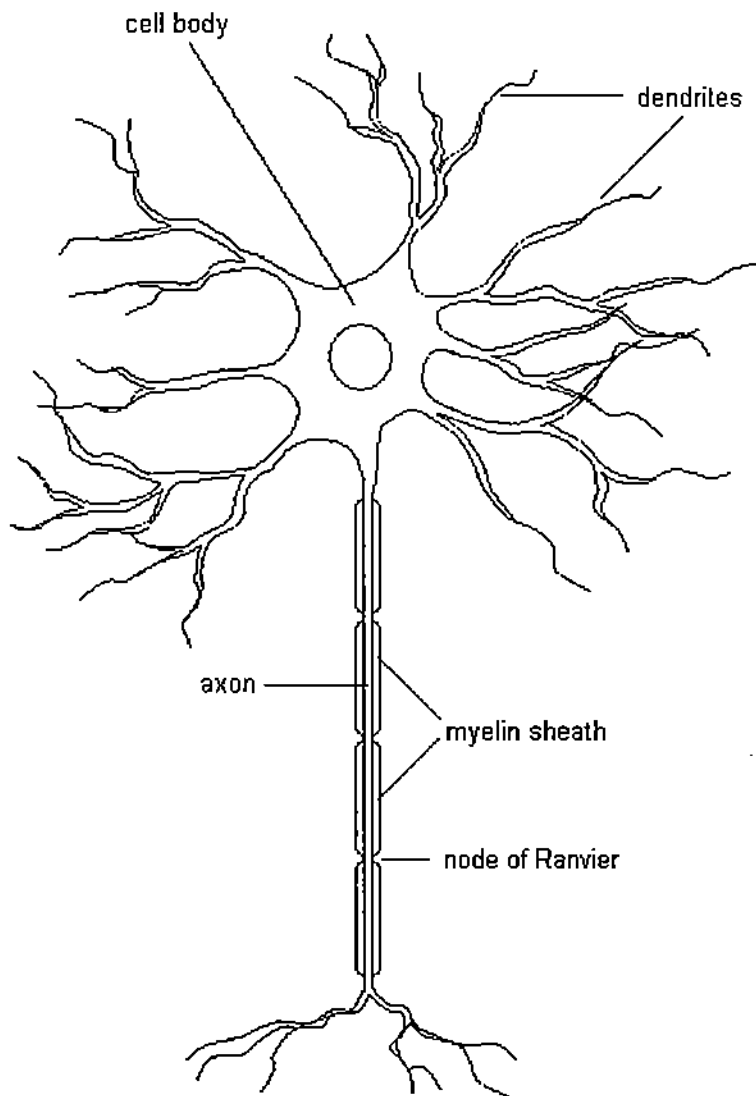| Pathology	Points
Myelin	1
Axoplasm	2
Periaxonal Space	
25 - 49%	4
50 - 74%	6
$\geq 75\%$	10
Necrotic Axoplasm	10

Figure 1: Schematic diagram of a neuron

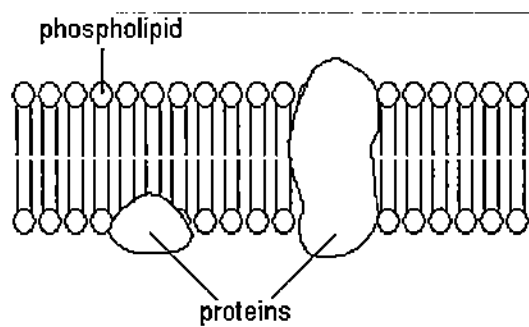Figure 2: Schematic diagram showing the cross-section of a plasma membrane

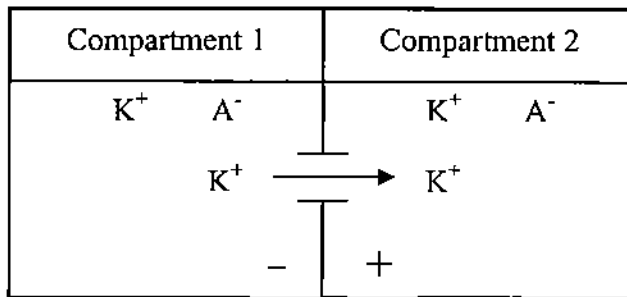Figure 3: Schematic example of ionic flux across a plasma membrane

Compartment 1	Compartment 2
K^+ A^-	K^+ A^-
K^+ $\longrightarrow$	K^+
$-$	$+$

Figure 4: Schematic diagram of the Na^+-K^+ ATPase pump

$3\ Na^+$

Extracellular compartment

Intracellular compartment

$2\ K^+$

Figure 5: Graph of an action potential

mV

+30

depolarization   repolarization

0

hyperpolarization

threshold

-70   equilibrium

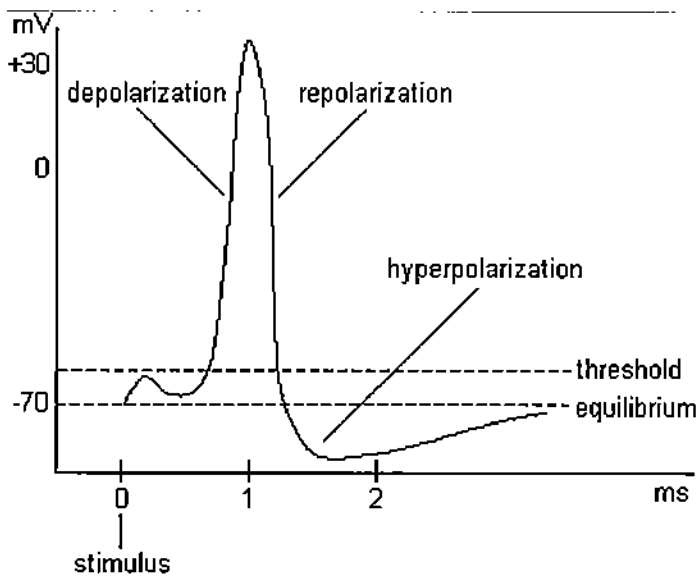0   1   2   ms

stimulus

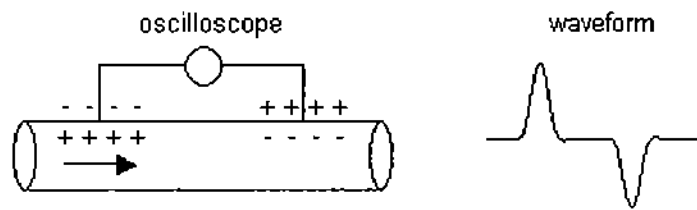25

Figure 6: Diphasic External Recording of an Action Potential

Figure 7: Diphasic External Recording of an Action Potential